Proceedings of the American Control Conference
Albuquerque, New Mexico June 1997
0-7803-3832-4/97/$10.00 © 1997 AACC

4D Air Traffic Control for Non-4D-Equipped Aircraft

M. R. Jardin
jardin@osprey.arc.nasa.gov
NASA Ames Research Center
MS 210-9
Moffett Field, CA 94035

Abstract

Current concepts for 4-dimensional (4D) time-based air traffic control automation systems are generally designed to control aircraft so that they cross a final control waypoint at a scheduled time, but the trajectory between the initial waypoint and the control waypoint is not explicitly specified. Instead of this type of single-point 4D control, it may be advantageous to use closed-loop control to reference 4D trajectories. The design of a compensator to help air traffic controllers and pilots accurately and efficiently control aircraft to buffered 4D reference trajectories is presented in this paper. The main technical challenge is to develop a control algorithm that efficiently achieves 4D control for aircraft while maintaining acceptable air traffic controller workload levels. The approach is to soften 4D trajectory clearances by allowing aircraft to be within a well-defined error buffer region around the trajectory and to try and synchronize advisory updates with the reference trajectory advisories such that the aircraft remains within the buffer. A bias estimator is used to remove steady-state errors. The control algorithms are developed and a simple example of a 4D control scenario is presented.

Introduction

The aim of the present work is to describe a method for controlling non-4D-equipped aircraft to within specified error tolerances of reference 4D trajectories for use in air traffic control (ATC) automation systems. A non-4D-equipped aircraft is one that does not have onboard automation capabilities for closed-loop control to a reference 4D trajectory (3-dimensional position vs. time). Since the control loop must be closed through the communication of the pilot and air traffic controller, either by voice communication or by monitoring data-linked advisories, a requirement of any 4D control algorithm is that the number of control advisories be held to a reasonable level. Some background on the current state of time-based air traffic control automation will now be given.

Time-based ATC automation systems generally only require that an aircraft meet a time at a single control waypoint while some depend upon closed loop control to reference 4D trajectories. Algorithms for installation in onboard Flight Management Systems (FMS) have been developed which can provide accurate 4D control based upon well-known optimal control formulations [1,2], but a practical air traffic management system must also handle non-4D-equipped aircraft, at least for the foreseeable future [3]. This may be accomplished either by providing larger separation buffers for non-4D-equipped aircraft, or by providing automation tools to enable air traffic controllers to enhance the performance of non-4D-equipped aircraft.

The basic approach that has been taken for time-based ATC automation has been to use high-fidelity trajectory prediction software to compute aircraft trajectories which meet crossing restrictions at a final control waypoint, including a scheduled time of arrival (STA). Trajectory solutions are iterated upon until a trajectory is found that meets the crossing restrictions, and the resulting control commands for that trajectory (headings, top-of-descent points, segment airspeeds) are then displayed for the air traffic controller to issue to the pilots. Time-based air traffic control automation systems such as CTAS (Center-TRACON Automation System) [5], TIMER (Traffic Intelligence for the Management of Efficient Runway-scheduling) [6], and similar systems developed in Europe [7,8] have provided 4D guidance capabilities for non-4D-equipped aircraft by using this method and have demonstrated arrival time accuracies of about ±20 seconds for delivery of aircraft from the end of the cruise segment of flight to metering fixes at the entrance to the Terminal Radar Approach Control (TRACON) area [5]. Since this method only seeks to achieve an arrival time at a final waypoint, conflict prediction and resolution functions must continually be performed on the resulting trajectories to ensure that conflicts between aircraft do not occur. This type of 4D control is closed-loop with regard to the end-point arrival time because new trajectory advisories are continually being generated as the aircraft executes a trajectory and encounters perturbations (primarily atmospheric). Depending upon atmospheric conditions and other flight parameters, however, aircraft may get into situations in which the STA becomes impractical and inefficient so that some aircraft must be rescheduled and assigned new arrival times.

The rescheduling of aircraft is certainly feasible, but it is undesirable for a system that must operate with both

4D-equipped and non-4D-equipped aircraft because much of the benefit of using on board 4D guidance equipment is lost if rescheduling is required. In addition, the continuous rescheduling of aircraft and the required conflict prediction and resolution functions are difficult tasks for the ground-based automation system to perform. For these reasons, it may be beneficial to develop algorithms that can regulate non-4D-equipped aircraft to within some specified tolerance of a 4D reference trajectory. This type of control to reference 4D trajectories will be called 4D reference control as opposed to the 4D STA control discussed previously. If 4D reference control is used, all conflict resolution tasks may be performed as a one-time strategic planning task, perhaps as part of a global optimization scheme so that no additional conflict resolution or rescheduling would be required.

Two approaches have been taken in the past towards developing this type of 4D control. A manual approach has been devised for systems in which a mix of 4D-equipped and unequipped aircraft operate together where the air traffic controllers use the 4D aircraft as guideposts to help vector the unequipped aircraft [3]. Simulations of this approach suggested that computer generated advisories might be necessary to improve the performance of the non-4D-equipped aircraft so that airport capacity and controller workload are not adversely affected. The second approach is a modification of 4D STA control where the problem is formulated as a discrete nonlinear optimal control problem so that the optimal reference trajectories that are generated are flown by having the air traffic controller (presumably through pilot/controller monitored data-link) issue regular discrete-time commands to each aircraft [9]. At the proposed sample rate of one command per aircraft each 30 seconds or so, the workload would certainly overwhelm both the pilots and air traffic controllers. The problem with a discrete-time formulation is that control commands are generated at fixed intervals whether they are needed or not. This forces an unnecessary trade-off to be made between system performance/stability and pilot/controller workload.

This paper presents a method for generating control advisories only when they are needed. In the proposed scheme, the 4D reference trajectory is computed as accurately as possible using current state-of-the-art trajectory generators, and then the purpose of the control system is to keep the aircraft to within some specified tolerance of the reference trajectory. Closed-loop control is achieved by using the predicted control advisories as feed-forward commands and then relying on feedback to close the 4D control loop and remove the effects of modeling uncertainties and system perturbations.

Problem Definition

In this preliminary treatment, the aircraft is assumed to be under closed-loop control in airspeed and in the three spatial dimensions, either by a 3D-equipped FMS and autopilot, or manually, so that the control problem is effectively reduced to one spatial dimension (along-track). Manual control may not be as precise as FMS control so that one might expect larger and more frequent speed control advisories to be issued to manually controlled aircraft, but the control principles that will be described are the same in any case. The dynamic modeling of the system, including the feed-forward linearization, will now be presented.

Referring to the 4D guidance speed control diagram (Fig.

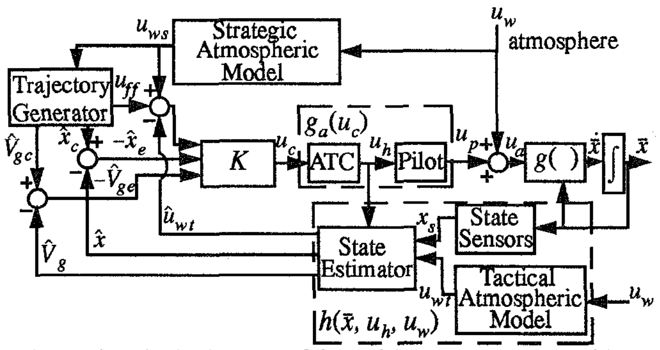

Figure 1. Block diagram of 4D guidance speed-control loop for non-4D FMS-equipped aircraft.

1), the modeled along-track wind speed (u_{ws}) is input to the Trajectory Generator function (Fig. 2) which uses the modeled

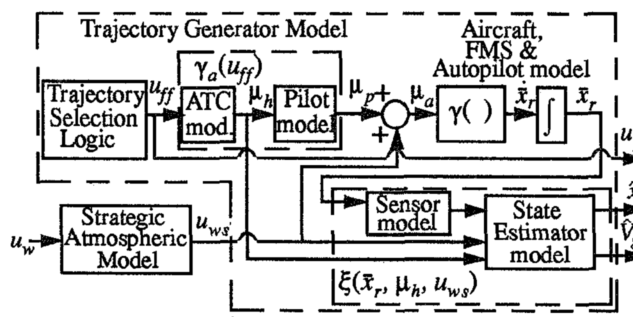

Figure 2. Block diagram of the Trajectory Generator function.

winds, aircraft dynamic model, and trajectory profile (route, airspeed, altitude constraints) to generate an accurate 4D command trajectory. The command trajectory consists of the predicted along-track measured position ($\hat{x}_c$), the along-track measured ground-speed ($\hat{V}_{gc}$), and the corresponding control advisory airspeeds (u_{ff}). The Trajectory Generator functions may be performed either by the air-based or ground-based system, or by a combination of both such that the resulting trajectory is preference-optimal in some sense (fuel or arrival time, for instance) and is also conflict free [1,2]. In a typical electro-mechanical system, if the reference trajectory represents the real trajectory closely enough to keep the trajectory error in a linear region, then linear control design techniques may be successfully employed. In this case, however, the control actuation is performed through communication between the air traffic controller and the pilot so that it is more critical that a very accurate and realistic trajectory generator be employed.

The reference trajectory created by the Trajectory Generator (Fig. 2) may be written in terms of the modeled system dynamics as

$$\dot{\bar{x}}_r = \gamma(\bar{x}_r, [\gamma_a(u_{ff}) + u_{ws}]) \tag{1}$$

where $\bar{x}_r$ is the reference state vector, u_{ff} is the reference airspeed input, u_{ws} is the along-track wind speed from the strategic wind model, $\gamma_a(u_{ff})$ is a function representing the model of the ATC and pilot dynamics, and $\gamma(\bar{x}_r, [\gamma_a(u_{ff}) + u_{ws}])$ is a function representing the model of the dynamics of the aircraft, pilot and human ATC systems. Similarly, the actual aircraft, pilot and human ATC dynamics (Fig. 1) may be written as

$$\dot{\bar{x}} = g(\bar{x}, [g_a(u_c) + u_w]) \tag{2}$$

where $\bar{x}$ is the state vector, u_c is the airspeed command, u_w is the along-track wind speed, $g_a(u_c)$ is a function representing the actual ATC and pilot dynamics, and $g(\bar{x}, [\gamma_a(u_c) + u_w])$ is the function representing the true system dynamics of the aircraft, FMS and autopilot.

In order to write the system dynamics as linear functions of perturbation quantities, the Taylor Series expansion of Eq. (2) is written as

$$\dot{\bar{x}} = g(\bar{x}_r, [\gamma_a(u_{ff}) + u_{ws}]) + \left[\frac{\partial g}{\partial \bar{x}}\right]\Delta\bar{x} + \left[\frac{\partial g}{\partial u}\right]\Delta u + \bar{\varepsilon} \tag{3}$$

where $\Delta\bar{x} = \bar{x} - \bar{x}_c$, $\Delta u = g_a(u_c) - \gamma_a(u_{ff}) + u_w - u_{ws}$, and $\bar{\varepsilon}$ is a vector consisting of the higher order terms of the expansion.

Subtracting Eq. (1) from Eq. (3) gives the following linearized equations for the state vector perturbations

$$\Delta\dot{\bar{x}} = \left[\frac{\partial g}{\partial \bar{x}}\right]\Delta\bar{x} + \left[\frac{\partial g}{\partial u}\right]\Delta u + \bar{\varepsilon}_g \tag{4}$$

where $\bar{\varepsilon}_g$ is a vector representing the higher order expansion terms.

Following a similar procedure, the perturbation sensor output equations can be written as

$$\Delta\bar{z} = \left[\frac{\partial h}{\partial \bar{x}}\right]\Delta\bar{x} + \left[\frac{\partial h}{\partial u}\right]\Delta u + \left[\frac{\partial h}{\partial u_h}\right]\Delta u_h + \bar{\varepsilon}_h \tag{5}$$

where in this case, the perturbation output vector is defined as

$$\Delta\bar{z} = \begin{bmatrix} \hat{x}_e \\ \hat{V}_{ge} \\ \hat{u}_{we} \end{bmatrix} \tag{6}$$

and $\bar{\varepsilon}_h$ is a vector representing the modeling errors and higher order series expansion terms.

The next step is to make the appropriate feedback connections (Fig. 1). The estimated aircraft along-track position and ground speed are fed back and subtracted from the reference inputs from the Trajectory Generator, and the estimated along-track wind speed, $\hat{u}_{wt}$, is fed back and subtracted from the strategic model of the wind speed, u_{ws} to achieve bias error cancellation. With these connections, the command airspeed, u_c, is given by

$$u_c = K(-\hat{x}_e, -\hat{V}_{ge}, [u_{ff} - \hat{u}_{we}]) \tag{7}$$

where the function $K(\ )$ represents the compensator. Since u_{ff} is the reference airspeed command, the compensator will be designed such that u_{ff} is generally just fed straight through without modification or time delay so that Eq. (7) may be well approximated by

$$u_c = K(-\hat{x}_e, -\hat{V}_{ge}, -\hat{u}_{we}) + u_{ff} \tag{8}$$

By restricting the ATC and pilot dynamics to linear functions we may write

$$g_a(u_c) = g_a(K(-\hat{x}_e, -\hat{V}_{ge}, -\hat{u}_{we})) + g_a(u_{ff}) \tag{9}$$

The along-track wind speed may be written as the sum of the estimated wind speed and a disturbance in the following way

$$u_w = \hat{u}_{wt} + \varepsilon_w \tag{10}$$

so that $\hat{u}_{we}$ may be written as

$$\hat{u}_{we} = u_w - u_{ws} - \varepsilon_w = \delta u_w - \varepsilon_w \tag{11}$$

Substituting Eqs. (9) through (11) into the previously given expression for Δu then gives

$$\Delta u = g_a(K(-\hat{x}_e, -\hat{V}_{ge}, [-\delta u_w + \varepsilon_w])) + \delta u_w + \varepsilon_a \tag{12}$$

where ε_a is the controller/pilot modeling error and is given by

$$\varepsilon_a = g_a(u_{ff}) - \gamma_a(u_{ff}) \tag{13}$$

The perturbation equations of motion are now obtained by substituting Eq. (12) into Eq. (4). The block diagram representation of the perturbation equations (Fig. 3) shows how the control system is a simple regulator driven solely by the various disturbances and the strategic wind error, δu_w. Since the ATC and pilot blocks have unity gain (they are modeled as pure

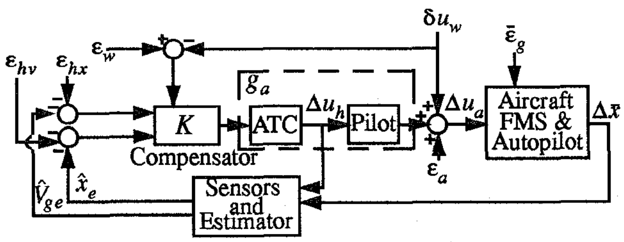

Figure 3. Block diagram of perturbation equations for 4D guidance speed-control loop.

time delay), and since the compensator will operate on the wind error with unity gain, the strategic wind error will approximately cancel so that this source of bias error can be removed.

It is possible in this case to develop a very simple and accurate dynamic model for this system so that phase-plane techniques may be used for the design of the compensator. When under the control of a pilot or an autopilot, the aircraft ground speed response may be well modeled as a first-order lag. With the assumption that the sensor and estimator dynamics have higher time constants than that of the aircraft, the transfer functions for $\hat{x}_e$ and $\hat{V}_{ge}$ representing the linearized system dynamics of Eqs. (4) & (5) may be approximated by

$$\frac{\hat{V}_{ge}(s)}{\Delta u_a(s)} = \frac{a}{(s+a)} \text{ and } \frac{\hat{x}_e(s)}{\Delta u_a(s)} = \frac{a}{s(s+a)} \tag{14}$$

where $\Delta u_a \equiv u_a - \mu_a$.

As previously mentioned, the ATC and pilot functions may be modeled as pure time delays, and these delays will be directly accounted for within the compensator.

Compensator Design

The feedforward advisories computed by the Trajectory Generator must be issued to keep the aircraft along the commanded reference trajectory, so these will be issued independently of any tactical advisories that become necessary due to the various perturbations. The primary means for minimizing the number of tactical control advisories is to try and synchronize them with the feedforward advisories in such a way that the aircraft will remain within some specified error buffer of the reference trajectory. The size of the error buffers may be determined based upon the variances of the trajectory perturbations so that a good balance is achieved between system performance and pilot/controller workload. In this case, system performance is to be measured in terms of achievable minimum aircraft spacing. The approach to designing the compensator is to determine analytical expressions describing the perturbation phase plane trajectories so that these expressions may be used to define limiting regions in the phase plane and so that tactical advisories may be computed that, when issued coincident with the strategic advisories, will keep the aircraft within the error buffer.

In addition to the feedforward commands, the output of the compensator must either be set and held to $-\delta u_w$ at time $t = \tau$ (aircraft is within error buffer so that only bias cancellation is needed) or must be set and held to the sum of a computed advisory and the wind error for bias cancellation as shown here

$$K(-\hat{x}_e, -\hat{V}_{ge}, -\delta u_w) = \begin{cases} -\delta u_w & \text{bias cancellation} \\ f(-\hat{x}_e, -\hat{V}_{ge}, \tau) - \delta u_w & \text{bias cancel. \& advisory} \end{cases} \tag{15}$$

where $f(-\hat{x}_e, -\hat{V}_{ge}, \tau)$ is a tactical clearance that is computed by the compensator independently of the bias cancellation clearance, δu_w.

From Eq. (14), the differential equation governing the plant dynamics may be written as

$$\frac{d\hat{V}_{ge}}{d\hat{x}_e} \cdot \hat{V}_{ge}(t) + a \cdot \hat{V}_{ge}(t) = -\lambda(t) \tag{16}$$

where

$$\lambda \equiv a \cdot K(\hat{x}_e, \hat{V}_{ge}, \delta u_w) - a \cdot \delta u_w \tag{17}$$

Note that the ATC/pilot function, $g_a(\ )$, has been left out of Eq. (17) at this time. As noted earlier, this function is modeled as a pure time delay, and this will later be explicitly accounted for within the compensator logic.

For convenience, the units of time may be normalized with the following definition

$$\theta = a \cdot t \tag{18}$$

so that Eq. (16) may be written as

$$\frac{dy}{dx} \cdot y(\theta) + y(\theta) = -\Lambda(\theta) \tag{19}$$

where

$$\Lambda(\theta) = \frac{\lambda(\theta)}{a^2} \tag{20}$$

and

$$x \equiv \hat{x}_e \text{ and } y \equiv \frac{dx}{d\theta} \tag{21}$$

From Eqs. (15), (17), and (20), Λ is given by the following expressions

$$\Lambda = \begin{cases} \varepsilon(\theta) & \text{bias cancellation} \\ \frac{1}{a} \cdot f(\hat{x}_e, \hat{V}_{ge}, \tau) + \varepsilon(\theta) & \text{bias cancel. \& advisory} \end{cases} \tag{22}$$

where

$$\varepsilon(\theta) = \frac{1}{a} \cdot [\delta u_w(\tau) - \delta u_w(\theta)] \tag{23}$$

For phase plane analysis, Eq. (19) may be solved in terms of x and y for the cases where Λ is either zero or nonzero. The case where Λ is zero simply leads to

$$(y - y_0) = -(x - x_0) \tag{24}$$

which defines a family of linear characteristics which end on the x-axis (Fig. 4). The nonzero case leads to

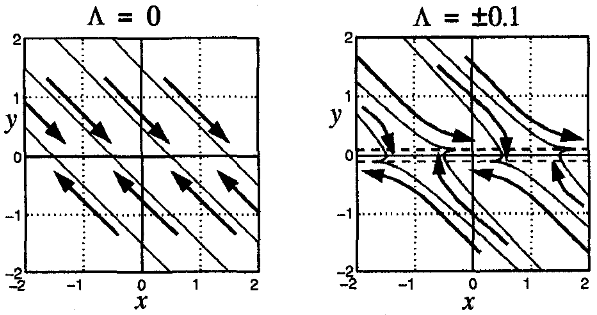

Figure 4. Characteristics of $\frac{dy}{dx} \cdot y + y = -\Lambda$ for $\Lambda = 0$ and $\Lambda = \pm 0.1$

$$(x - x_0) = -\left[(y - y_0) - \Lambda \cdot \ln\left(\frac{\Lambda + y}{\Lambda + y_0}\right)\right] \tag{25}$$

The characteristics for this case asymptotically approach lines of $y = -x$ away from the x-axis, but then approach lines of constant y at a value of y equal to the ground speed error so that the phase trajectories will come in from the far regions of the phase plane to follow a line of constant y parallel to the x-axis off towards infinity (Fig. 4).

The error buffers may be plotted in the phase plane to study how the logic in the nonlinear function will have to work in order to minimize the number of control advisories while keeping the aircraft within the buffer (Fig. 5). The error buffer which the aircraft must physically stay within will be called the Absolute Error Buffer (AEB) and is represented by the region between two vertical lines on the phase plane. Depending upon the nature of the error buffer that is used, the AEB may or may not be centered about the origin, and the position of the AEB may or may not vary with time. Control advisories must be issued before the AEB is reached because if control advisories are not issued until the AEB is reached, then the control advisory communication delay might cause the aircraft to drift beyond the buffer before control action can be taken. The region in the phase plane which defines the limits of where control advisories must be issued will be referred to as the Control Error Buffer (CEB). The CEB is a dynamically defined region which depends upon where the aircraft is in the phase plane, the particular characteristic being followed, and

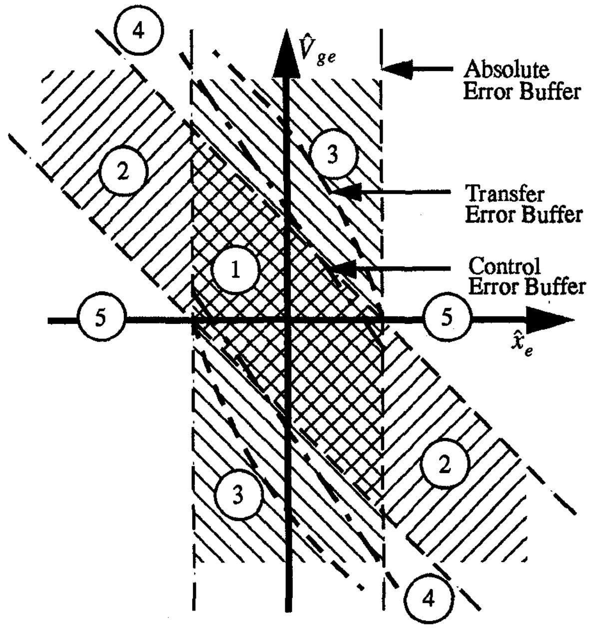

Figure 5. Five regions of the phase plane representing the system $\frac{dy}{dx} \cdot y + y = 0$ and idealized representations of the three error buffers.

the amount of time before the next strategic advisory is scheduled. Within the CEB is another region called the Transfer Error Buffer (TEB) which is the limit of where control advisories must be *executed* (not just *issued*) in order to take the aircraft to the desired final trajectory. These buffer regions will now be explored in greater detail.

For the case where $\Lambda = 0$, five regions may be identified (Fig. 5). In region 1, no control advisories are required since the aircraft starts inside the AEB and will reach a steady-state that will be inside the error buffer for all time. In region 2, the aircraft starts outside of the AEB but will end up inside of the AEB in a finite amount of time and will remain there in the steady state so that one might decide not to issue any control advisories. In region 3, the aircraft begins within the AEB but will drift outside of the AEB in a finite amount of time into region 5 and will remain outside of the AEB in the steady state. Depending upon the situation, one may or may not decide to issue an advisory from region 3. In region 4, the aircraft starts outside the AEB but will enter region 3, and region 5 has the aircraft outside of the AEB for all time.

For the case where Λ is nonzero, such as when a tactical advisory is in effect or there is an error between the previous bias cancellation advisory and the current wind bias, the characteristics all asymptotically approach lines of constant, nonzero ΔV_g. Since the aircraft will ultimately end up outside of the AEB for the nonzero Λ case, there are no regions comparable to regions 1 and 2 of the $\Lambda = 0$ case.

The important cases to treat here are when the aircraft starts within region 3 for $\Lambda = 0$ or within regions 3 or 4 for nonzero Λ. Since this control system is being developed to keep the aircraft within the AEB, the aircraft should not be allowed to venture far into region 5. If the aircraft were to end up in this region, some form of renegotiation of the strategic trajectory clearance or a special tactical advisory would be required to bring the aircraft into region 1 or 3. Similarly, the aircraft should not be allowed to venture far into region 2, but for small incursions into this region, the $\Lambda = 0$ trajectories would automatically bring the aircraft into region 1 so that no special treatment is required. For small incursions into region 4, the aircraft also will automatically enter region 3 so that no special treatment is required here either.

For the two regions within the AEB, regions 1 and 3, we may now calculate the CEB limits. The goal of the following calculations is to determine the limiting regions of the phase plane where it is still possible to wait for the next strategic advisory before issuing a tactical advisory and still remain within the AEB. This problem is most easily worked backwards from the desired final trajectory. The desire is to end up on a $\Lambda = 0$ trajectory that will take the aircraft to a steady state within region 1 defined by

$$y = -x + b \tag{26}$$

where b is ideally set to zero so that the final trajectory will take the aircraft back to the center of the AEB. However, a less restrictive CEB may be defined using $b = \pm x_{AEB}$ because this defines the limit of where a $\Lambda = 0$ trajectory will remain within region 1. The constraint that the trajectory must not breach the AEB in the process of arriving at the final trajectory will also be used to obtain an analytical expression for the CEB. Finally, the communication delay will be accounted for to define the true limits of the CEB.

A set of equations may be solved for the initial coordinates of a trajectory that begins at the time of the n^{th} strategic advisory and that will intersect the final trajectory precisely at the time the $(n+1)^{th}$ strategic advisory is scheduled to occur. The transfer trajectory equation is obtained by solving Eq. (19) to get

$$x_{n+1} = -\Lambda_n \cdot \Delta\theta_s + x_n + (y_n + \Lambda_n)(1 - e^{-\Delta\theta_s}) \tag{27}$$

which, when differentiated, gives the corresponding equation for y

$$y_{n+1} = y_n \cdot e^{-\Delta\theta_s} + \Lambda_n(e^{-\Delta\theta_s} - 1) \tag{28}$$

where the subscripts 'n' and '$(n+1)$' refer to quantities at the time of the n^{th} and $(n+1)^{st}$ strategic advisories and $\Delta\theta_s$ is defined by

$$\Delta\theta_s \equiv \theta_{n+1} - \theta_n \tag{29}$$

and it is assumed that the advisory communication delay, $\Delta\theta_d$, at the $(n+1)^{st}$ strategic advisory has been accounted for within $\Delta\theta_s$.

Writing Eq. (26) with $y = y_{n+1}$ and $x = x_{n+1}$ and combining with Eqs. (27) & (28) forms a set of three linear algebraic equations which may readily be solved for x_{n+1}, y_{n+1} and Λ_n in terms of x_n and y_n. For now, we are most interested in Λ_n which is given by

$$\Lambda_n = \frac{x_n + y_n - b}{\Delta\theta_s} \tag{30}$$

The final constraint that the trajectory not breach the AEB may be expressed by writing Eq. (25) with x_0 and y_0 replaced with x_n and y_n and setting $x = x_{AEB}$ and $y = 0$. The resulting equation

$$x_{AEB} = x_n + y_n + \Lambda_n \cdot \ln\left(\frac{\Lambda_n}{\Lambda_n + y_n}\right) \tag{31}$$

may be combined with Eq. (30) and rearranged to give

$$e^{[(x_{AEB} - b)/\Lambda_n]} = \frac{\Theta \cdot \Lambda}{\Lambda + y_n} \tag{32}$$

where

$$\Theta \equiv e^{\Delta\theta_s} \tag{33}$$

The solution to Eq. (32) may be expressed in closed-form as

$$\Lambda_n = \frac{-(x_{AEB} - b)}{\left[\frac{(x_{AEB} - b)}{y_n} - L_w\left(\Theta \cdot \frac{(x_{AEB} - b)}{y_n} \cdot e^{[(x_{AEB} - b)/y_n]}\right)\right]} \tag{34}$$

where Lambert's w-function, $L_w(\ )$ [10], has been introduced and is defined such that $w = L_w(x)$ is the solution to $w \cdot e^w = x$. Referring back to Eq. (22), the compensator output is formed by adding this computed value of Λ_n to the bias cancellation value, $\frac{1}{a}\delta u_w$.

Combining Eq. (34) with Eq. (30) gives the following equation for x_n as a function of y_n

$$x_n = \frac{-\Delta\theta_s(x_{AEB} - b)}{\left[\frac{(x_{AEB} - b)}{y_n} - L_w\left(\Theta \cdot \frac{(x_{AEB} - b)}{y_n} \cdot e^{[(x_{AEB} - b)/y_n]}\right)\right]} + b - y_n \tag{35}$$

and this is the definition of what will be referred to as the Transfer Error Buffer (TEB) because the curve defined by this function will take the aircraft from the TEB to the desired final trajectory.

The final calculation required to define the CEB is to account for the initial communication delay and the time from the initial position until the time of the n^{th} strategic advisory. The curve defined by this calculation will be the limit of where a tactical advisory may be given at the time of the next scheduled strategic advisory (the n^{th} advisory) such that by the time the tactical advisory is executed, the initial trajectory will intersect the TEB and take the aircraft to the desired final trajectory.

Combining Eqs. (27) and (28) for the initial values of $x = x_i$, $y = y_i$, and $\Lambda = \Lambda_i$ so that the initial delay-induced trajectory segment ends at $x = x_n$ and $y = y_n$ after a delay time of $\Delta\theta_d$ and solving for x_i leads to

$$x_i = x_n + \Lambda_i \cdot \Delta\theta_d + (y_n + \Lambda_i)(1 - e^{\Delta\theta_d}) \tag{36}$$

and

$$y_i = [y_n - \Lambda_i(e^{-\Delta\theta_d} - 1)]e^{\Delta\theta_d} \tag{37}$$

which, along with Eq. (35) are the desired expressions for the CEB.

The control procedure is to use Eqs. (35), (36) & (37) along with appropriate values of x_{AEB}, b, $\Delta\theta_s$, $\Delta\theta_d$, and Λ_i to compute x_i and y_i as functions of the dependent variable, y_n. These values of x_i and y_i define the boundary of the CEB so that one may compare the current aircraft position and velocity with the CEB region. As long as the aircraft remains within the CEB, 4D reference control may be achieved by simply modifying the feedforward control advisories so that no additional advisories are required. The amount that the feedforward advisories must be modified is given by the sum of Λ_n from Eq. (34) and any bias cancellation that is required. However, if the CEB is breached, then a tactical control advisory will be required prior to the time of the next scheduled feedforward advisory. Depending upon the particular situation, several options are available. For example, if the next feedforward advisory is scheduled soon relative to the current time, it may be possible to modify the advisory and then issue it earlier than planned. If this is not possible, then an additional tactical advisory can be issued. The timing of the additional tactical advisory should be made so that it does not come so close to the following scheduled feedforward advisory that it is not possible for the controller to issue both commands consecutively.

4D Control Simulation Example

The definitions for the error buffers may now be illustrated with a simple 4D control scenario. The buffers and the resulting aircraft trajectory will be plotted for a case where the aircraft is initially in region 1 of the phase plane when an uncompensated wind speed error of about 2.5 m/s (5 knots) develops that puts the aircraft on a trajectory that will ultimately breach the AEB. For this case, an initial communication delay of 15 seconds is assumed, and the time between strategic advisories is 5 minutes (including communication delay for the final strategic advisory). The aircraft model transfer function for this example is governed by Eq. (14) with $a = 0.085s^{-1}$ which is the approximate reduced-order transfer function for a large jet like the Boeing 747. The AEB in this case has been set to 900 meters and the desired final trajectory has been chosen to take the aircraft back to the center of the AEB.

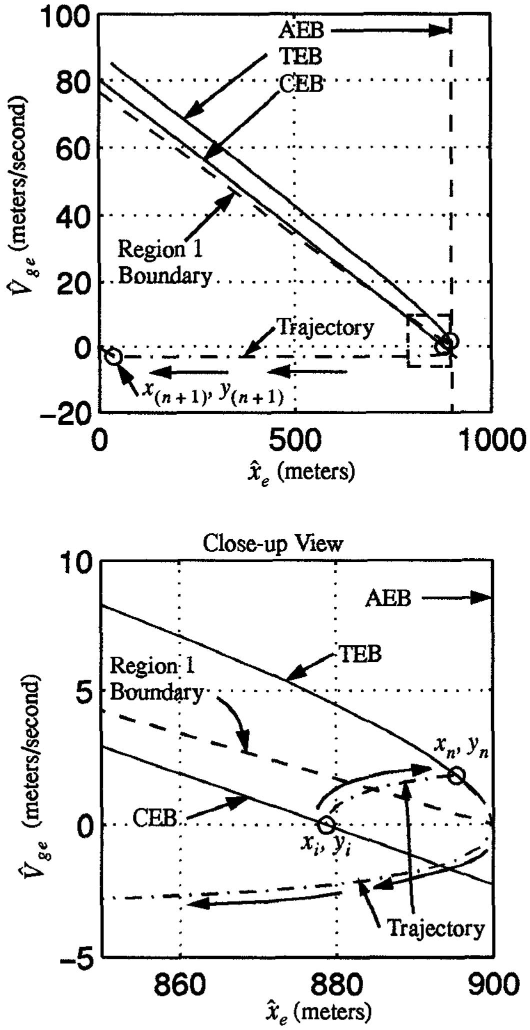

Figure 6. Advisory-minimized tactical trajectories in the $\hat{x}_e$ - $\hat{V}_{ge}$ phase plane and the associated error buffers.

The resulting buffers are plotted along with the resulting trajectory for the conditions stated above (Fig. 6). The larger scale plot shows that the trajectory does end up on the characteristic that takes the aircraft back to the center of the AEB while the finer scale plot shows how the trajectory proceeds from the CEB to the TEB.

The position and velocity errors are also plotted vs. time (Fig. 7) to show the time scales for this problem. Notice that,

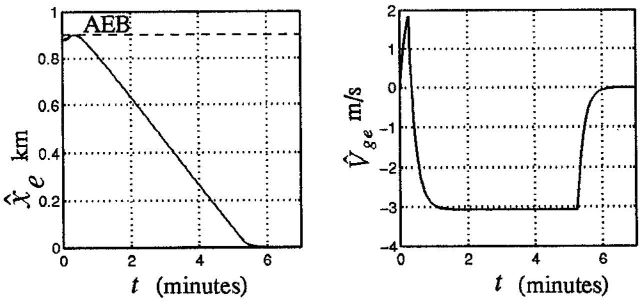

Figure 7. Position and ground-speed errors vs. time.

as designed, the first tactical advisory occurs after the 15 second communication delay to put the aircraft on the transfer trajectory which then takes precisely 5 minutes to put the aircraft on the final trajectory which brings it to the center of the AEB.

Conclusions

A phase-plane technique for designing a nonlinear compensator to minimize the number of required tactical control advisories for 4-dimensional human-in-the-loop air traffic control has been presented. The logic for the proposed compensator seeks to synchronize any necessary tactical control advisories with existing strategic control advisories so that pilot/controller workload is reduced. In order to make a practical system, error buffers have been introduced which allow the aircraft to drift in a small region surrounding their strategic trajectory clearance so that continuous control advisories are not needed.

The simplified case of speed-only control has been used to illustrate the compensator design techniques. The aircraft transfer function from commanded airspeed to ground speed has been modeled as a simple first order lag, and the resulting dynamic equations have been solved in order to be used in the advisory minimization calculations of the compensator. The concept of the three different error buffers, the AEB, TEB, and CEB and the equations defining them have been presented. A simple example was then used to demonstrate how the developed compensator might work in practice.

References

[1] Lidén, S., "Optimum 4-D Guidance For Long Flights," IEEE/AIAA 11th Digital Avionics Systems Conference, 1992.

[2] Erzberger, H., and Chapel, J. D., "Concepts and Algorithms for Terminal Area Traffic Management," American Control Conference, June 1984, San Diego, CA.

[3] Tobias, L., Erzberger, H., Lee, H. Q., O'Brien, P. J., "Mixing Four-Dimensional Equipped and Unequipped Aircraft in the Terminal Area," *AIAA Journal of Guidance, Control, and Dynamics*, Vol. 8, No. 3, May-June 1985, pp. 296-303.

[4] Erwin, R. L., and Izumi, K. H., "Use of 4D RNAV in Time-Based *En Route* Arrival Metering," AGARD-AG-301, Vol. 2, May 1990, pp. 28-1 - 18-19.

[5] Erzberger, H., Davis, T. J., and Green, S., "Design of Center-TRACON Automation System," AGARD-CP-538, pp. 11-1 - 11-12, May 1993.

[6] Credeur, L., and Capron, W. R., "A Description and Evaluation of 'TIMER' -- A Time-Based Terminal Flow-Control Concept," AGARD-AG-301, Vol. 2, May 1990, pp. 27-1 - 27-42.

[7] Adam, V., and Kohrs, R., "On Board Planning of 4D-Trajectories," AGARD-CP-504, 1992, Amsterdam, The Netherlands, Oct. 22-24, 1991, pp. 16-1 - 16-12.

[8] Benoît, A., and Swierstra, S., "Next Generation of Control Techniques in Advanced TMA: Automatic Assistance for the Controller/Pilot Dialogue," AGARD-CP-401, Brussels, Belgium, 1986, pp. 55E-1 - 55E-15.

[9] Nagarajan, N., "Four-Dimensional Guidance Problem with Control Delays," *AIAA Journal of Aircraft*, Vol. 13, No. 8, August, 1976, pp. 559-564.

[10] Corless, R. M., Gonnet, G. H., Hare, D. E. G., and Jeffrey, D. J., "Lambert's W-Function in Maple," and "On Lambert's W-Function," both available as technical reports from the Dept. of Applied Math., Univ. of Western Ontario, London, Ontario, Canada.